ISSN 0965-545X, Polymer Science, Series A, 2017, Vol. 59, No. 1, pp. 107–115. © Pleiades Publishing, Ltd., 2017.
Original Russian Text © A.E. Chalykh, U.V. Nikulova, A.A. Shcherbina, V.V. Matveev, 2017, published in Vysokomolekulyarnye Soedineniya, Seriya A, 2017, Vol. 59, No. 1, pp. 86–94.

POLYMER BLENDS

Phase Equilibria in a Polyethylene–Polystyrene System

A. E. Chalykh, U. V. Nikulova, A. A. Shcherbina*, and V. V. Matveev

Frumkin Institute of Physical Chemistry and Electrochemistry, Russian Academy of Sciences, Leninskii pr. 31, Moscow, 119991 Russia

**e-mail: aachalykh@mail.ru*

Received April 20, 2016;
Revised Manuscript Received June 14, 2016

Abstract—The method of optical interferometry is used to study the interaction of PE with PS in situ. On the basis of the obtained data, phase diagrams of the PE–PS system are constructed for a number of molecular masses of the components. For PE and PS oligomers, the UCMT values are determined. Pair parameters for the interaction of homopolymers are calculated, and their dependences on temperature and molecular mass are considered. The quantitative analysis of the behavior of high-molecular-mass fractions of PE and PS at high temperatures is carried out, and the regions of a partial compatibility of the components are predicted.

DOI: 10.1134/S0965545X17010023

INTRODUCTION

The structure and properties of PE–PS blends have been investigated for several decades [1–7]. An engineering reason for the production of PE–PS blends was the desire to increase the hardness of PE, its impact strength, flexibility, and transparency and to decrease its shrinkage. In accordance with these requirements, systems for investigation were selected on the basis of variation in their molecular masses, MMD, and branching type [6, 8]. Careful attention was paid to revealing specific features of the formation of a heterogeneous structure of one of the polymers in the other one and its changes under various processing and operation conditions.

The blends of PE and PS exhibit typical features of macromolecular incompatibility [8], with their structure being either spherolites or fibrils of one component in the matrix of the other one or structures of the type matrix–inclusion which are described for melts of polymer blends. The rheology of these systems has been studied most fully [9–15]. It was shown that extreme points are observed on the dependences of rheological and operating properties of these composites on their compositions. Their appearance is assigned to mass-exchange processes that occur within interphase layers of mcroheterogeneous systems [6].

In order to control heterogeneity, a third component was added to these blends, namely, the block copolymers of styrene with butadiene, plasticizers, and polyolefin copolymers that promote an increase in adhesion, reduction in shrinkage, and enhancement of flowability and wettability [16, 17]. In [6], PS–polyethylenebutylene block copolymer was used as a compatibilizer of PE–PS blends. This made it possible to obtain composites with a uniform distribution of the PS dispersed phase in the PE matrix and high stress–strain properties.

The crystallinity of PE blended with PS decreases upon an increase in the content of PE [12], while its melting temperature changes in the range of 404–409 K [18, 19]. In the presence of the compatibilizer, the melting temperature of the PE phase is in the range of 402–407 K. This fact is explained by both the sizes of crystallites and the dissolution of polyolefin blocks in the PS matrix.

It is commonly believed that PE and PS are incompatible [20–24]. However, in solutions of xylene and toluene, which are common solvents for both indicated polymers, PS–PE blends are mutually soluble at a temperature of 363 K and a mass ratio of 1 : 1 [7]. It was shown that structural changes of the blends during prolonged observations are accompanied by "homogenization" processes which lead to the redistribution of sizes of dispersed phase particles and the formation of branched structures [18, 19]. It was assumed that these effects are caused by the partial compatibility and diffusion of macromolecules for which the driving force is the thermodynamic instability of microheterogeneous blends. The partial compatibility of blend components is confirmed by the migration of PS into the PE matrix during graft polymerization [25]. In [5], an attempt was made to construct the phase diagram for blends of PE and PS oligomers.

For progression of these ideas, it was of interest to extend the range of measurements and to study in detail phase equilibria and interdiffusion in the PE–

Table 1. Characteristics of the objects of research

Polymer	Manufacturer	$M_w \times 10^{-3}$	MMD	T_g^*, K	T_m^*/T_{cr}^*, K
PS-1	Aldrich	0.82	1.11	303	–
PS-2	PSS	1.18	1.07	343	–
PS-3	Aldrich	2.33	1.07	348	–
PS-4	Waters Associates	9.0	1.01	373	–
PE-1	Fluka	1.11	1.11	208	387 / 377
PE-2	Fluka	17.0	1.38	229	407 / 390
PE-3	Fluka	60.0	1.48	231	406 / 389
PE-4	Fluka	153.0	1.72	231	405 / 389

* Determined by DSC and optical interferometry.

PS system in a wide range of temperatures and molecular masses of the components. This was the aim of the present study.

EXPERIMENTAL

In the present work, low-molecular-mass fractions of PS with $M = (0.8–9.0) \times 10^3$ and PE with $M = (1.11–153.0) \times 10^3$ were used. The characteristics of the used polymers are listed in Table 1.

The solubility and interdiffusion of the polymers were studied in the temperature range of 370–500 K by optical interferometry on an ODA-2 laser diffusiometer [26, 27]. A helium-neon laser with a wavelength of 632 nm was used as a light source. The interferential pattern was recorded on a computer using a PAL/SECAM video camera.

The technique of measurements did not differ from the traditional one [26, 28]. A PE film 100–150 μm thick was placed in a diffusiometer cell that was a planar wedge-shaped glass capillary. The film was preliminarily prepared from the melt of polyolefin granules at $T_m + 40$ K.

After thermostatting at the given temperature, the capillary was filled with the PS melt. The moment of contact between the components which was registered by the electron-optical system of the interferometer was taken as the start of the interdiffusion process.

The measurements were conducted in the step-by-step mode of temperature increase and decrease in the range of 280–500 K. The time of thermostatting at each step was at least 70 min. For every cycle of temperature increase and decrease, the compositions of coexisting phases were determined.

In preliminary experiments, temperature dependences of the refractive indexes of PS and PE were measured (Fig. 1) and further used to determine the compositions of coexisting phases. The data for PE (Fig. 1, curve *1*) are taken from [29].

For example, for PS-1 at temperatures above T_g (415 K), the difference in the refractive indexes is 0.1006; this value corresponds to 33 stripes on interferential patterns. This means that the refractive index increment per stripe is 0.003, and the concentration is measured with an accuracy of up to 2.98%.

The DSC method was used to determine the glass-transition and melting temperatures of homopolymers. Measurements were carried out on a DCS 204F1 Phoenix (Netzsch) device at a heating rate of 10 K/min in the range of 295–450 K.

RESULTS AND DISCUSSION

Typical interferential patterns of transition zones of conjugated PE and PS phases are presented in Fig. 2. It is seen that, at an experiment temperature of T_c of polystyrene $< T < T_m$ of polyolefin, the transition region includes the zone of gradient solutions corresponding to the dissolution of crystalline polyolefin in the PS melt (Fig. 2a, region IV) and interface (Fig. 2a, region III). Near this interface, the saturated solution of PE (φ_1') in the PS melt is formed and preserved throughout the observation time. This solution corresponds to the coexistence of PE crystals with solution, namely, the melt of PE in PS. Regions I and II are assigned to pure components.

At $T > T_m$ of PE, the interdiffusion zone changes to a certain extent (Fig. 2b). Under these conditions, this zone is the superposition of three regions: interface (III) and the zones of solubility of PE in PS (IV) and of PS in PE (V). Under isothermal annealing conditions, concentration jump φ_1'/φ_1'', corresponding to the compositions of coexisting phases, is spontaneously formed and preserved near the interface. With increasing temperature (Fig. 2c), the concentration

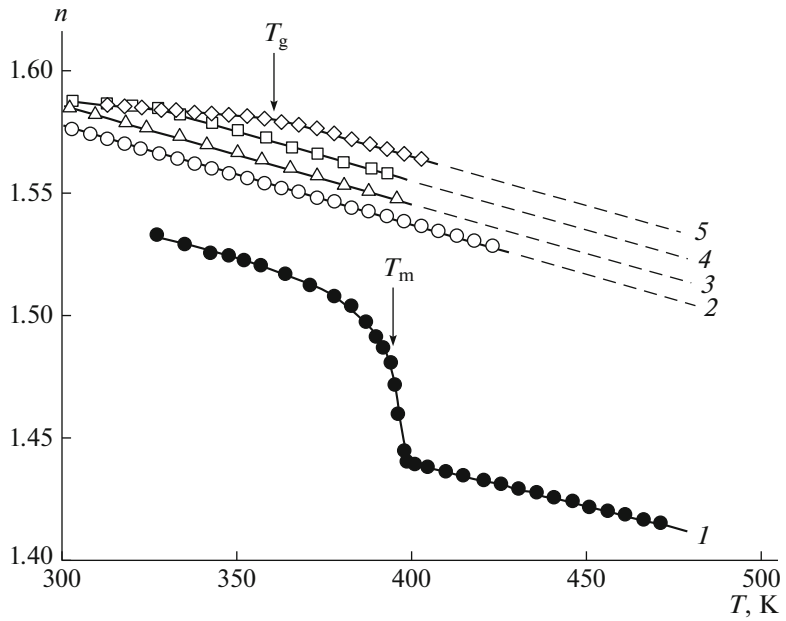

Fig. 1. Temperature dependence of the refractive index for (*1*) PE with $M_w = 3 \times 10^4$, (*2*) PS-1, (*3*) PS-2, (*4*) PS-3, and (*5*) PS-4.

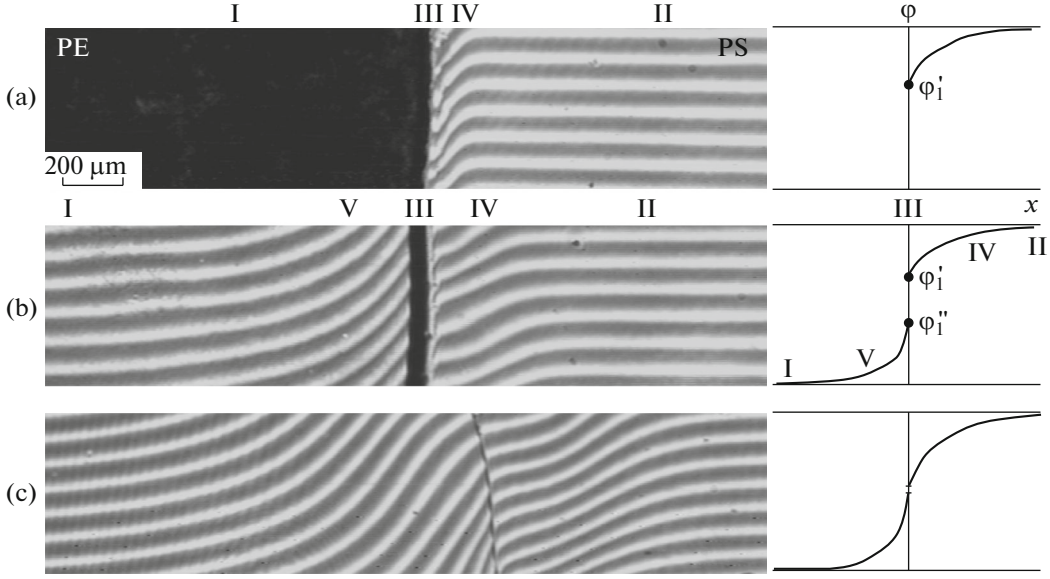

Fig. 2. Interferential patterns of interdiffusion zones in the system PE–PS at (a) 383, (b) 393, and (c) 433 K. Here and in Figs. 3 and 4, the molecular masses of polyethylene and polystyrene are $M_w = 1.11 \times 10^3$ and 1.18×10^3, respectively. φ_1' and φ_1'' are the compositions of coexisting phases.

jump at the interface becomes less pronounced, and the interface disappears at $T > 433$ K. At this temperature, the conjugated phases of PE and PS melts are mutually soluble, and the transition zone corresponds to a single-phase gradient solution within which the composition changes smoothly on transition from one component to the other one.

The step-by-step cooling of this gradient system (Fig. 3a) leads to the sequential formation of the concentration profile of the interface within a certain range, with the position of the interface coinciding with the position of UCMT on the diagram, and then to the amorphous delamination of supersaturated solutions on both sides of the interface (Figs. 3b, 3c,

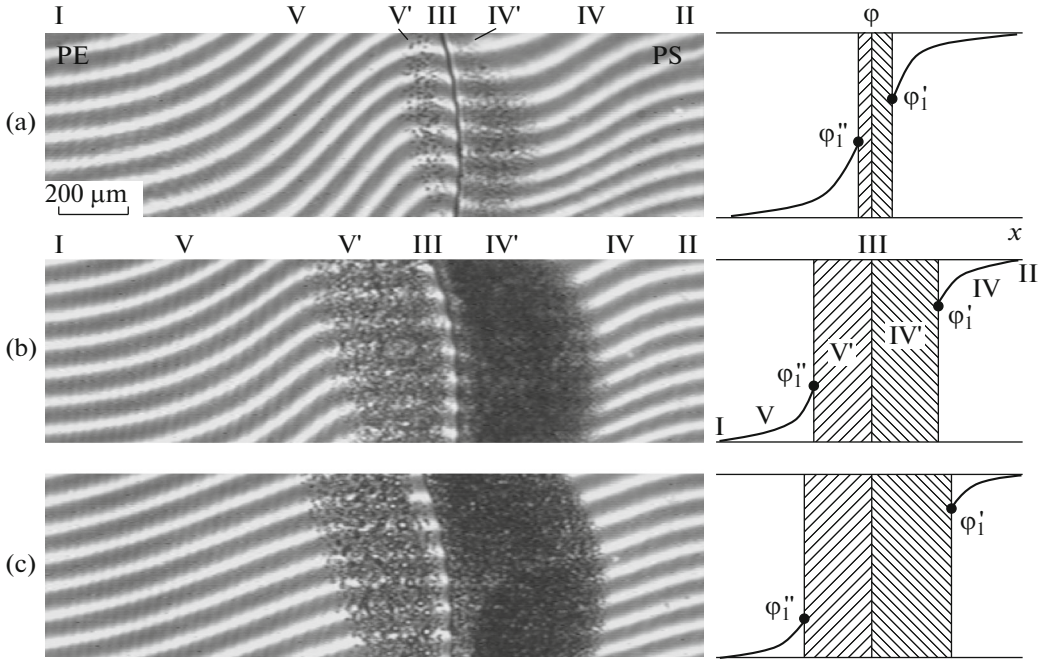

Fig. 3. Interferential patterns of interdiffusion zones in the system PE–PS formed upon step-by-step decrease in temperature to (a) 418 and (b) 393 K and (c) treated at 393 K for a certain time.

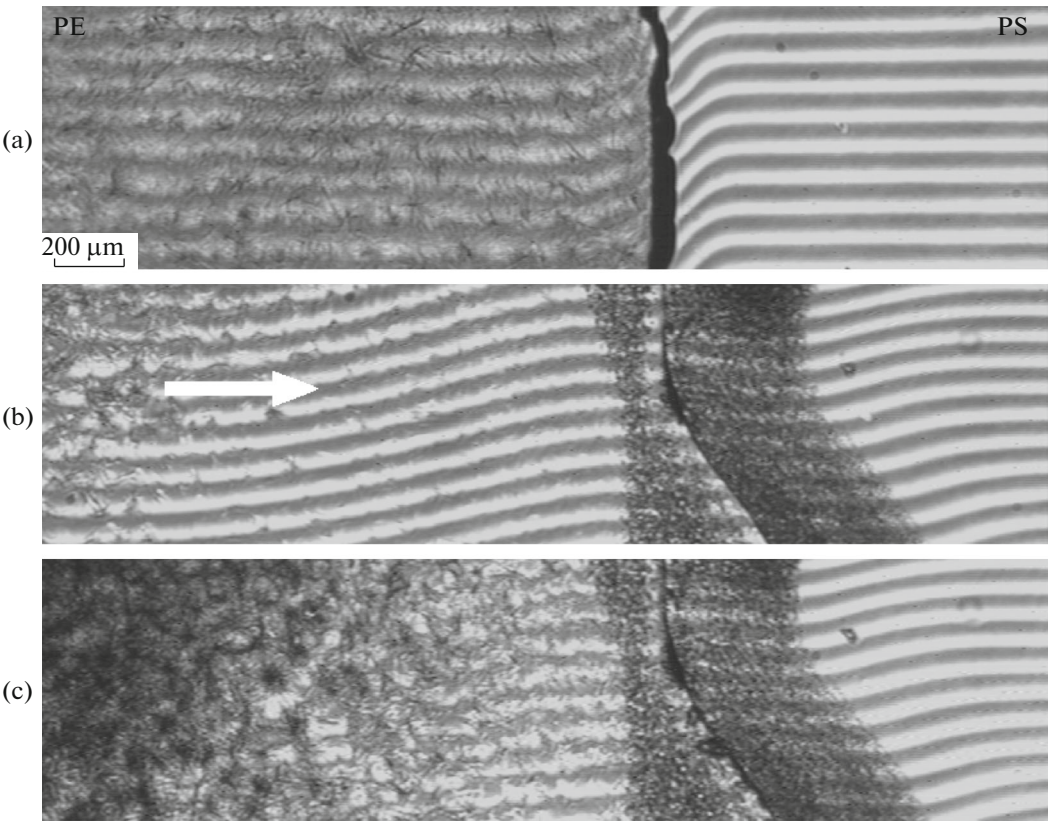

Fig. 4. The structure of transition zones in the system PE–PS obtained at a temperature of 388 K (a) under the heating regime and (b, c) under the cooling regime. Explanations are given in the text.

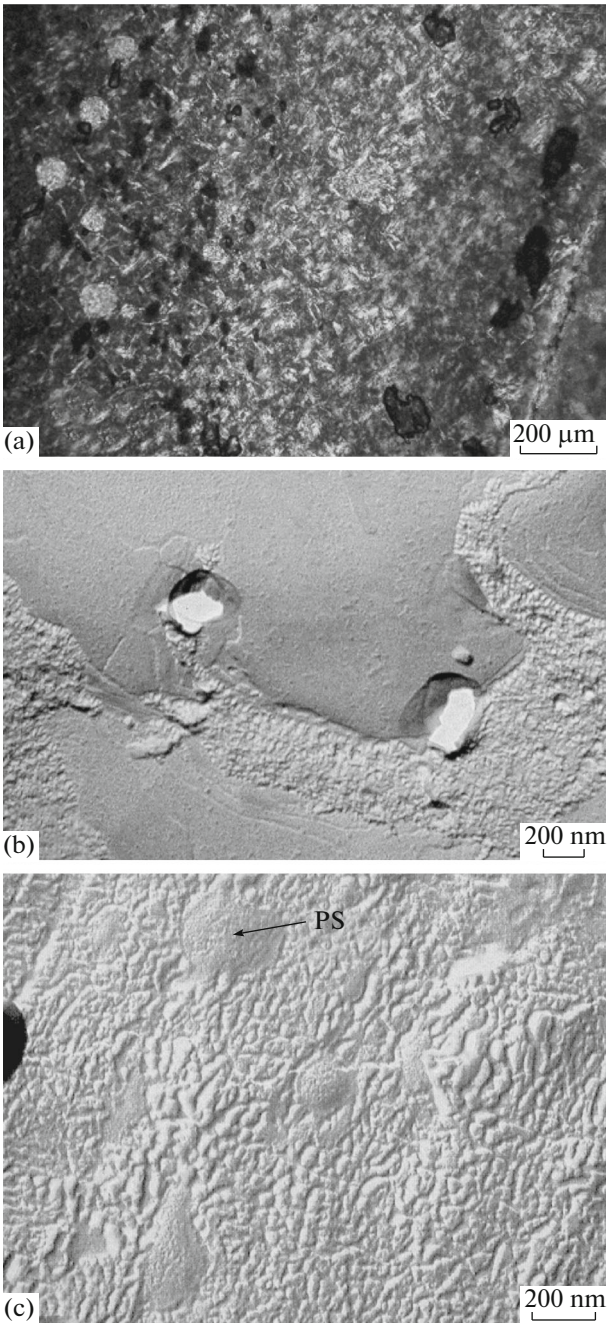

Fig. 5. (a) Surface micrographs of low-temperature cleaved surfaces of the transition zone of the system PE–PS obtained using a polarization optical microscope and (b, c) fragments of regions of this zone obtained using a transmission electron microscope. Explanations are given in the text.

regions IV' and V'), phase separation of dispersions, and formation of the macroscopic interface.

When a temperature of 383 K is reached, the process of PE crystallization starts (Fig. 4b). The crystallization front propagates along the diffusion direction (shown by the arrow), and the concentration profile

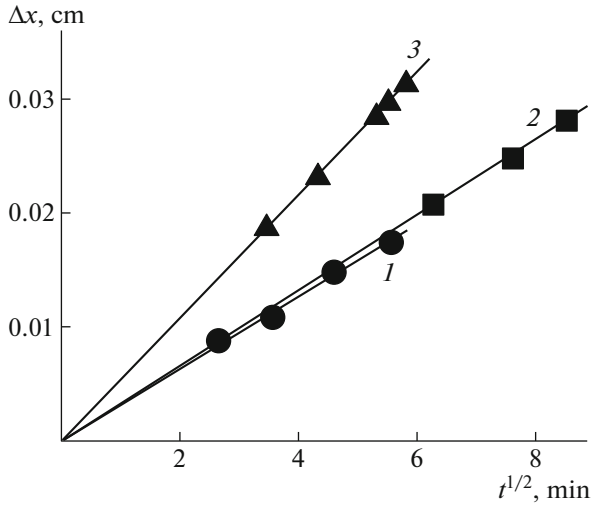

Fig. 6. Kinetics of the motion of isoconcentration planes in the system PE-1–PS-2.

changes owing to displacement of macromolecules of PS from its solutions in PE by growing polyethylene crystals. The crystallization process ends with formation of the macroscopic interface and dispersions of crystal PE particles in the PS matrix (Figs. 5a, 5b, on the right) and PS particles in the PE matrix (Fig. 5c, on the left) on both sides of the interface. Micrographs are taken from different regions of transition diffusion zones.

The kinetics of diffusion front motion in the system PE-1–PS-2 is presented in Fig. 6. It is clearly seen that, near the T_m of PE, the slope of straight lines changes weakly, since its changes are prevented by the crystalline state of PE (Fig. 6, lines *1*, *2*). At $T > T_m$ of PE, PE macromolecules acquire a high mobility and the interdiffusion rate increases (Fig. 6, line *3*).

On the basis of compositions of the coexisting phases, the phase diagrams of the PE–PS systems with different MM of the components were constructed (Figs. 7, 8).

The phase equilibrium in these systems is characterized by several specific features. Firstly, the general property of the studied binary systems is the combination of both crystalline and amorphous equilibria, the behavior of which in the diffusion zone of component mixing confirms the principle of mutual independence of phase equilibria. Secondly, an increase in the mutual solubility of thermoplastics with increasing temperature is observed. Despite the fact that the presence of UCMT was experimentally detected for only one particular system (PE-1–PS-1), it may be stated that all the blends are characterized by the diagrams of amorphous lamination with the UCMT. Because the components have close molecular masses, critical concentrations φ_{cr} are situated in the middle range of compositions, while experimentally

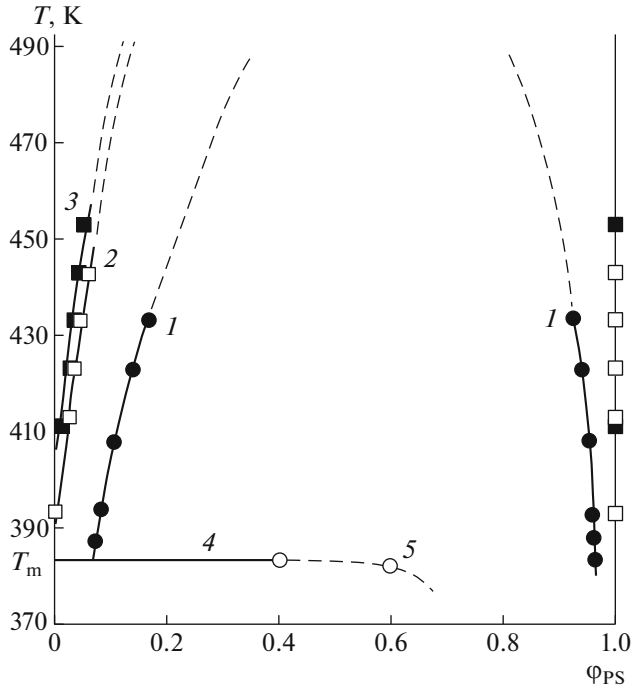

Fig. 7. Phase diagram of the system PE–PS. The molecular mass of polystyrene is $M_w = 1.18 \times 10^3$ and the molecular mass of polyethylene is $M_w \times 10^{-3} = (1)$ 1.11, (*2*) 17.0, and (*3*) 60.0. The melting temperature of the PE phase is determined from the data of (*4*) DSC and (*5*) interferometry.

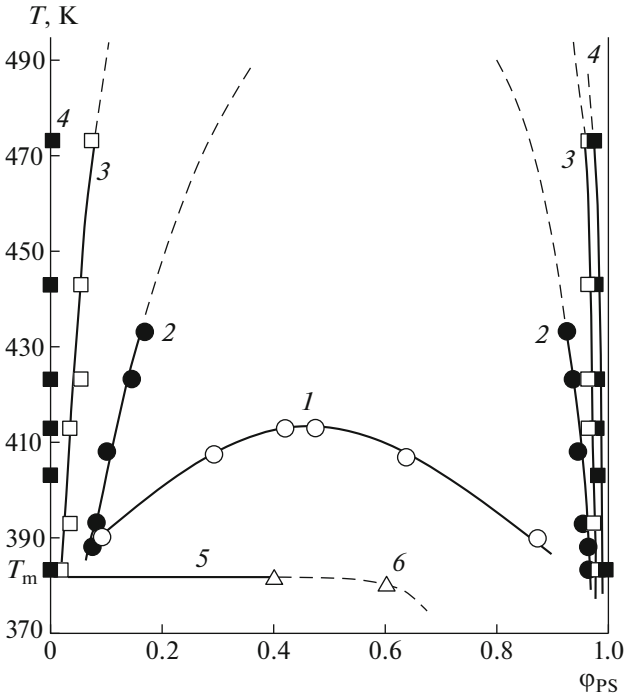

Fig. 8. Phase diagram of the system PE–PS. The molecular mass of polyethylene is $M_w = 1.11 \times 10^3$ and the molecular masses of polystyrene are $M_w \times 10^{-3} = (1)$ 0.82, (*2*) 1.18, (*3*) 2.33, and (*4*) 9.0. The melting temperature of the PE phase is determined from the data of (*5*) DSC and (*6*) interferometry.

found φ_{cr} values are closed to those calculated from the Flory–Huggins equation.

Finally, the parameters of binodal curves, namely, the critical points and the compositions of coexisting phases, depend on the molecular masses of the components. Moreover, the trend of changes in the diagram of amorphous lamination of the PE–PS system observed upon increase in their molecular mass corresponds to usual regularities: the higher the molecular masses of PS and PE, the lower the mutual solubility of the components, and the wider the range of the two-phase region. The effect of molecular mass on the mutual solubility of the components is the most pronounced on the isothermal cross sections of phase diagrams. The quantitative analysis performed upon extrapolation of the bimodal curves constructed in φ' (φ'')$-1/M_{PE}$ coordinates at $M_{PE} \to 0$ showed that the values of limiting solubility for PS-2 in the melt of high-molecular-mass PE vary in the range of 3–6 vol % as the temperature increases from 413 to 473 K.

Table 2. Parameters of critical points in the systems PE–PS

System	UCMT, K	φ_{cr} (experiment / calculation)
PE-1–PS-1	413*/418	0.45 / 0.692
PE-1–PS-2	495	0.64 / 0.650
PE-1–PS-3	606	0.57 / 0.571
PE-2–PS-1	600	0.87 / 0.879
PE-3–PS-1	606	0.93 / 0.932

* Experimental data for UCMT.

On the basis of compositions of the coexisting phases, the pair interaction parameters χ were calculated for the polymer blends as described in [30]. The temperature dependences of the indicated parameters are presented in Fig. 9. It is seen that, at $T > T_m$ of PE, the linear $\chi - 1/T$ dependence is observed for all the systems, and its extrapolation to critical χ_{cr} conditions makes it possible to obtain an additional estimate for the value of UCMT and critical compositions (Table 2). The nonlinear character of these dependences (curves *2*, *3*) corresponds to the temperature range below the crystallization of PE.

Figure 10 shows changes in the values of χ upon increasing the molecular masses of the components. It is seen that, as the molecular mass of PS increases, the values of χ vary according to similar curves with saturation. The largest changes occur within the oligomeric range of MM values. At $M > 2 \times 10^3$, the param-

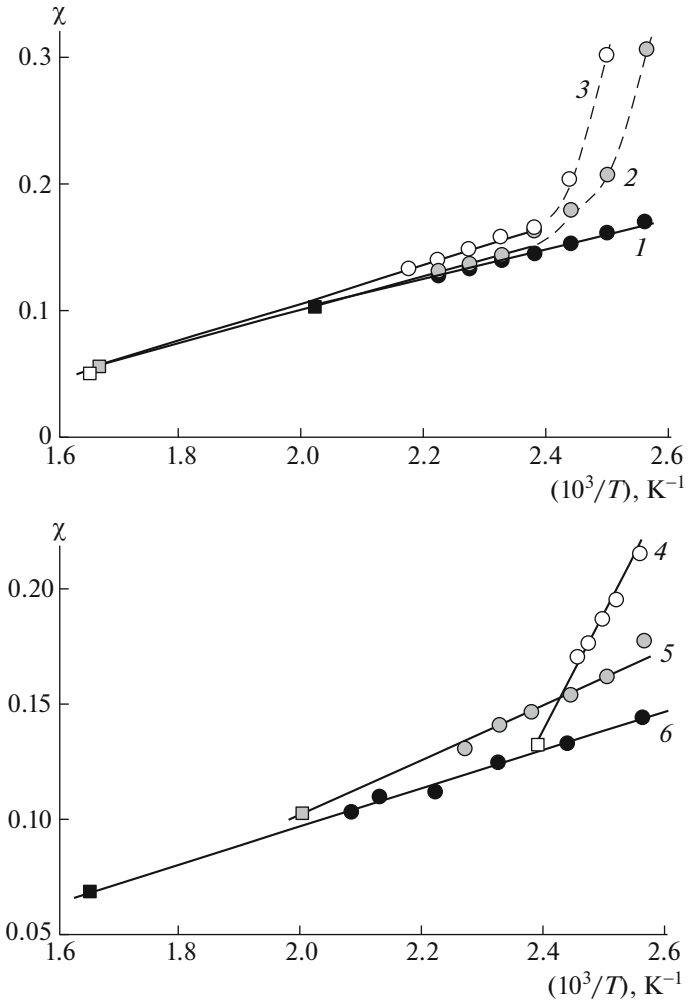

Fig. 9. Temperature dependence of the interaction parameter for the system PE–PS. (*1–3*) The molecular mass of polystyrene M_w = const = 1.18 × 10^3, and (*4–6*) the molecular masses of polyethylene M_w = const = 1.11 × 10^3. The molecular masses of the second component are $M_w \times 10^{-3}$ = (*1*) 1.11, (*2*) 17.0, (*3*) 60.0, (*4*) 0.82, (*5*) 1.18, and (*6*) 2.33.

eter χ asymptotically approaches a certain limiting value, which for high-molecular-mass fractions of thermoplastics changes within a rather narrow range of 0.13–0.14.

The approach developed in [30] makes it possible to solve both the direct problem, that is, to calculate pair solubility coefficients from the binodal curves of phase diagrams, and the inverse problem, that is, to obtain information boundary lines of amorphous lamination diagrams using temperature dependences of the parameter χ. The solution of the inverse problem made it possible to construct the generalized phase diagram (Fig. 11), on which not only binodal curves obtained from experimental data in the system PE-3–PS-2 (Fig. 11, curve *1*) but also the complete binodal bell, including the critical point (curve *2*) and the spinodal (curve *3*), are presented. These curves separate the temperature-concentration field into several characteristic zones: I is the region of homogeneous states, II is the region of metastable states, and III is the region of heterogeneous states. The diagram is also augmented by the data on the PE melting temperature (curve *4*). This makes it possible to identify the region of crystalline states (region IV). Additionally, the figure depicts the calculated data obtained for the spinodal of the high-molecular-mass PE–PS blend (curve *5*).

In the temperature range that is commonly used nowadays to process PE melts (above 500 K), a partial compatibility of the components at a level of ~5 vol % may be expected. However, it should be remembered that the system will undergo lamination accompanied by the formation of the above-described dispersed structures when the figurative point crosses the liquidus line.

Thus, the phase diagrams of the systems PE–PS are constructed for the first time. It is shown that the homopolymers are characterized by a partial compat-

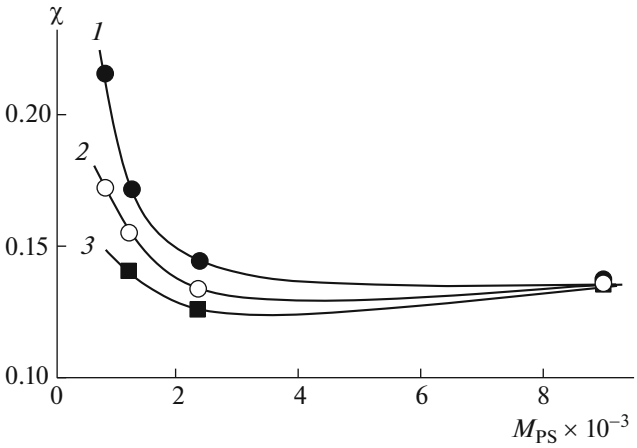

Fig. 10. Dependences of the parameter χ on the molecular mass of polystyrene. The molecular mass of polyethylene M_w is 1.11×10^3; the values of T are (*1*) 390, (*2*) 410, and (*3*) 430 K.

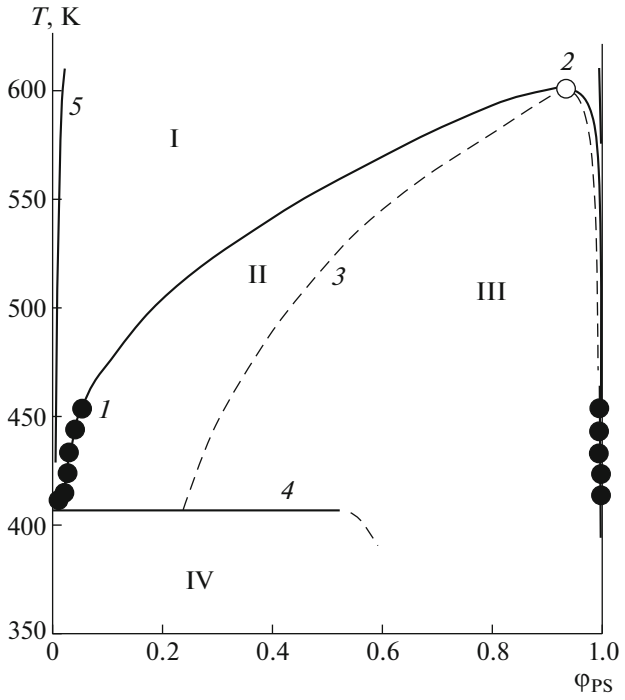

Fig. 11. Generalized phase diagram of the system PE-3–PS-2. (*1*) The binodal obtained from the experimental data, (*2*) the calculated parameters of the critical point, (*3*) the calculated data for the spinodal, (*4*) the melting temperature of PE-3, and (*5*) the calculated data for the spinodal in the system PE–PS for $M_{PE} = 153 \times 10^3$ and $M_{PS} = 60 \times 10^3$. I is the region of the homogeneous state of the system, II is the region of metastable states, III is the region of the heterogeneous state of the system, and IV is the region of crystalline states.

ibility and feature the UCMT. On the basis of the compositions of the coexisting phases, the values of the interaction parameter χ are calculated. Estimates of the solubility of PS and PE for a number of temperatures showed that the limiting solubility values are close to the numerical value of molecular mass for styrene. The obtained data make it possible explain the formation of grafted layers of PS on PE films by a good solubility of the oligomer components in each other.

ACKNOWLEDGMENTS

This work was supported by the Russian Foundation for Basic Research, project no. 14-03-00390.

REFERENCES

1. S. D. Sjoerdsma, A. S. A. M. Bleijenberg, and D. Heikens, in *Polymer Blends. Processing, Morphology and Properties,* Ed. by E. Martuscelli, R. Palumbo, and M. Kryszewscki (Plenum Press, New York; London, 1979), p. 201.
2. W. M. Barentsen and D. Heikens, Polymer **14**, 579 (1973).
3. W. M. Barentsen, D. Heikens, and P. Piet, Polymer **15**, 119 (1974).
4. D. Heikens and W. M. Barentsen, Polymer **18**, 69 (1977).
5. N. I. Puchkov, Candidate's Dissertation in Chemistry (IFKh RAN, Moscow, 1983).
6. *Polymer Blends,* Ed. by D. R. Paul and S. Newman (Acad. Press, London, 1978), Vol. 2.
7. O. Olabisi, L. M. Robeson, and M. T. Shaw, *Polymer-Polymer Miscibility* (Acad. Press, New York, 1979).
8. *Polymer Blends. Performance,* Ed. by D. R. Paul and C. B. Bucknall (Wiley, New York, 2000), Vol. II.
9. J. K. Kim, S. Kim, and C. E. Park, Polymer **38** (9), 2155 (1997).
10. N. D. B. Lazo and C. E. Scott, Polymer **40** (20), 5469 (1999).
11. J. Reignier and B. D. Favis, Macromolecules **33** (19), 6998 (2000).
12. S. Okamoto and H. Ishida, Macromolecules **34** (21), 7392 (2001).
13. T. Kallel, V. Massardier-Nageotte, M. Jaziri, J.-F. Gerard, and B. Elleuch, J. Appl. Polym. Sci. **90** (9), 2475 (2003).
14. B. Lin, F. Mighri, M. A. Huneault, and U. Sundararaj, Macromolecules **38** (13), 5609 (2005).
15. R. Salehiyan, Y. Yoo, W. J. Choy, and K. Hyun, Macromolecules **47** (12), 4066 (2014).
16. Z. Wang, C.-M. Chan, S. H. Zhu, and J. Shen, Polymer **39** (26), 6801 (1998).
17. R. Fayt, R. Jerome, and Ph. Teyssie, J. Polym. Sci., Part B: Polym. Phys. **27** (4), 775 (1989).
18. C. Harrats, R. Fayt, R. Jerome, and S. Blacher, J. Polym. Sci., Part B: Polym. Phys. **41** (2), 202 (2003).
19. G. Chen, S. Guo, and H. Li, J. Appl. Polum. Sci. **86** (1), 23 (2002).
20. *Polymer Blends,* Ed. by D. R. Paul and S. Newman (Acad. Press, London, 1978), Vol. 1.
21. V. N. Kuleznev, *Polymer Blends* (Khimiya, Moscow, 1980) [in Russian].

22. R. J. Kern and R. J. Slocombe, J. Polym. Sci. **15** (79), 183 (1955).
23. S. Krause, J. Polym. Sci., Part A-2: Polym. Phys. **7** (1), 249 (1969).
24. D. J. Dunn and S. Krause, Polym. Lett. Ed. **12** (10), 591 (1974).
25. A. E. Chalykh, V. K. Gerasimov, A. D. Aliev, V. V. Matveev, N. V. Shevlyakova, M. G. D'yakova, and V. A. Tverskoi, Polym. Sci., Ser. A **52** (4), 453 (2010).
26. A. Ya. Malkin and A. E. Chalykh, *Diffusion and Viscosity of Polymers: Measurement Techniques* (Khimiya, Moscow, 1979) [in Russian].
27. A. E. Chalykh, A. I. Zagaitov, D. P. Korotchenko, and V. V. Gromov, *Optical Diffusiometer* (IFKh RAN, Moscow, 1996) [in Russian].
28. A. E. Chalykh, U. V. Nikulova, and A. A. Shcherbina, Polym. Sci., Ser. A **57** (4), 445 (2015).
29. R. R. Khasbiullin, Candidate's Dissertation in Chemistry (IFKh RAN, Moscow, 2003).
30. A. E. Chalykh, V. K. Gerasimov, and Yu. M. Mikhailov, *Phase State Diagrams of Polymer Systems* (Yanus-K, Moscow, 1998) [in Russian].

Translated by A. Yakimansky